Dilute-Solution Hydrodynamic Behavior of Poly(α-methylstyrene) in a Good Solvent

J. C. Selser

IBM Research Laboratory, San Jose, California 95193. *Received March 27, 1980*

ABSTRACT: The hydrodynamic and thermodynamic behavior of seven narrow-distribution, atactic poly(α-methylstyrene) (PαMS) samples in toluene at 25 °C and benzene at 30 °C (PCS only) were studied by using both photon correlation spectroscopy (PCS) and time-averaged light scattering (TALS). In the molecular weight range 5×10^3–10^6, changes in the slope of log–log plots of the chain self-diffusion coefficient, D_0, vs. chain molecular weight reveal that effectively monodisperse, atactic PαMS in a good solvent at room temperature undergoes a gradual transition in chain statistics from Gaussian to excluded-volume behavior. In the excluded-volume region, $M > 10^5$, D_0 scales as the negative 0.59 power of molecular weight, in good agreement with both the Flory prediction of $^3/_5$ and the recent renormalization group calculation of 0.588, while the interpenetration function, ψ, is constant at 0.140, comfortably situated in the middle of a number of predictions of its value. These results support the view that in terms of both its coarse thermodynamic and hydrodynamic behavior, the linear chain in a good solvent may be replaced by its respective equivalent hard spheres. The ratio of the values of the PαMS chain hydrodynamic radius to its radius of gyration was measured to be about 0.5, in reasonable agreement with the recently calculated value of 0.537. Finally, the behavior of the PαMS chain–chain hydrodynamic interaction parameter, k_D, was found to be best described by the treatment of Yamakawa. For solution concentrations expressed in volume fraction units, k_D^* was measured to be about 2.7, in reasonable agreement with the Yamakawa prediction of 2.5 ± 0.2.

Introduction

The size dependence of chain molecular weight of nonionic linear polymer chains in a good solvent continues to be a subject of both theoretical and experimental interest. This dependence is of the power-law type

$$R \sim M^{\nu} \tag{1}$$

and for chains sufficiently large to have a random-coil configuration in solution, ν increases from somewhat greater than 0.5 to $\simeq$0.6 with increasing chain molecular weight, M, as a consequence of chain swelling due to the gradual increase in the effect of intrachain excluded volume.[1] Oftentimes, R is either the chain hydrodynamic radius, R_H, or its radius of gyration, R_G. These related size parameters are not identical. R_G reflects the heavier weighting of more widely spaced pairs of chain segments than does R_H.[2,3] Consequently, the evolution of the molecular weight dependence of the two is somewhat different.[3,4]

With the recent introduction of powerful new analytical methods, principally by de Gennes and des Cloizeaux and co-workers (see ref 2, for example) interest in studying the dynamic behavior of dilute synthetic polymer solutions has been revitalized. This interest has been further enhanced by the advent of laser light scattering techniques which can be used to measure R_H in dilute polymer solutions. Because it is a noninvasive probe of spontaneous solution concentration fluctuations, the technique of photon correlation spectroscopy (PCS) is ideally suited to the investigation of the chain dynamics of such solutions.[5] In particular, the dependence of the polymer chain self-diffusion coefficient D_0, and thus R_H (see eq 4), on chain molecular weight and on chain concentration may be accurately and precisely determined. As a consequence, three issues of fundamental importance in understanding the dilute-solution behavior of linear polymer chains in a good solvent may be addressed.

The first concerns the detection of changes in ν with M and the identification of the general location of the onset of that region of polymer molecular weight wherein the dependence of D_0 on M can validly be described by a power law of the form

$$D_0 = CM^{-\nu} \tag{2}$$

for which $\nu \simeq 0.6$. For the purposes of this paper, this region is referred to as the "excluded-volume" region and its location marks the completion of the transition from the Gaussian statistical behavior of the chain to the characterization of chain statistics in terms of larger statistical elements called "temperature blobs".[6-8]

The second issue to be resolved is the actual value of ν in the excluded-volume region. Of additional interest is the comparison of R_H to R_G.

The third issue to be addressed is the behavior, in the excluded-volume region, of k_D—the so-called diffusion coefficient second virial coefficient

$$D(c) = D_0(1 + k_D c) \tag{3}$$

with c the polymer concentration in solution. Characterization of k_D provides both useful information about chain–chain interactions in dilute solution and helps identify which, if any, of a number of theoretical predictions of its behavior is most applicable to this type of system.

Recent studies of the dependence of R_H on M for polystyrene in a good solvent around room temperature have shown that for that system, the change in ν with M is very gradual and the excluded-volume region is not reached even for chain molecular weights of several millions.[7,9,10] In such systems, ν is measured to be $\simeq$0.55. An explanation for this behavior has been recently proposed by Weill and des Cloizeaux, who show that for polystyrene in benzene at room temperature, for example, the buildup of the excluded-volume effect is so gradual that a value of $\simeq$0.6 can only be expected for molecular weights well above the maximum molecular weights employed in these studies.[4] A very recent PCS measurement of polystyrene, up to a molecular weight of 40×10^6, in toluene at 20 °C found $\nu = 0.577$, however.[11]

Given these results, a reasonable next step is to study, as outlined earlier, an architecturally somewhat more complex linear polymer. For comparison purposes, poly(α-methylstyrene) in a good solvent was chosen for investigation. Both PCS and time-averaged light scattering (TALS) measurements were made on the PαMS system. The results of this study are presented in this paper.

Sample Preparation

Seven narrow molecular weight distribution PαMS samples were synthesized by the Pressure Chemical Co. of Pittsburgh, Pa.

0024-9297/81/2214-0346$01.25/0

Table I
PαMS Molecular Weight Measurement Results

SAMPLE NO.	GPC				LS	MO,VPO	
	$\bar{M}_Z \cdot 10^3$(g)	$\bar{M}_W \cdot 10^3$(g)	$\bar{M}_N \cdot 10^3$(g)	$\bar{M}_W/\bar{M}_N$	$\bar{M}_W \cdot 10^3$(g)	$\bar{M}_N \cdot 10^3$(g)	$\bar{M}_W/\bar{M}_N$
1	7.13 (8.12)	5.37 (6.43)	3.90 (4.71)	1.37 (1.37)	8.64	5.43	1.59
2	26.2 (25.3)	22.1 (23.0)	18.4 (20.4)	1.20 (1.13)	32.7	26.8	1.22
3	83.7	76.5	69.6	1.10	91.7	89.0	1.03
4	169.0	156.0	144.0	1.09	145.3	140.0	1.04
5	457.0	425.0	398.0	1.07	394.6	314.0	1.26
6	–	–	–	–	792.9	661.2	1.20
7	1100	953.0	845.0	1.10	976.4	887.4	1.10

These samples ranged in molecular weight from about 5000 to about 1 000 000. The tacticities of these samples were assessed by proton nuclear magnetic resonance and all were determined to be atactic.[12] Typical relative amounts of the different tactic forms were as follows: isotactic, 0.05; heterotactic, 0.40; syndiotactic, 0.55.

For the light scattering measurements, samples were dissolved in spectroscopic grade toluene by gentle shaking overnight on a wrist shaker. In addition, six of the seven samples were dissolved in spectroscopic grade benzene in the same way. PCS measurements of these six samples provided additional useful information and served as a check on the PCS toluene results. The maximum concentration of solutions used in the PCS measurements corresponded, approximately, to a PαMS chain center-to-center spacing greater than twice the chain radius of gyration. The maximum concentrations used in the TALS measurements were generally somewhat lower than those used in the PCS measurements. The R_G values used in these determinations were calculated from the results of an earlier TALS study of atactic PαMS samples in toluene at 25 °C.[13] All light scattering solutions were prepared in volumetric flasks that had been acid cleaned and then rinsed in solvent prior to use. Each dilution of each solution was injected into the PCS or TALS spectrometer sample cell through a 0.5-μm Fluoropore filter or two 0.22-μm Fluoropore filters (Millipore Corp.), respectively, to help rid them of dust. Both the PCS and the TALS PαMS measurements in toluene were made at room temperature (21–23 °C). The sample temperature was taken to be room temperature after about 20 min. A laboratory thermometer was used to measure temperature, and reading the thermometer resulted in an estimated temperature uncertainty of about 0.2 °C. The toluene diffusion coefficient results were then temperature and viscosity corrected to 25 °C, using the Stokes–Einstein equation

$$D_0 = k_B T/6\pi\eta_0 R_H \tag{4}$$

with k_B the Boltzmann constant, T the absolute temperature, η_0 the solvent viscosity, and R_H the hydrodynamic radius of the PαMS chains in solution. Thus

$$D_0^{(2)} = D_0^{(1)} \frac{T^{(2)}}{T^{(1)}} \frac{\eta_0^{(1)}}{\eta_0^{(2)}} \tag{5}$$

with superscript 1 indicating measurement conditions and superscript 2 corresponding to 25 °C. The PCS measurements in benzene were made at 30.0 ± 0.1 °C, using the sample cell thermal control system described in detail in ref 14.

Experimental Methods

The apparatus used in making the PCS measurements reported here is the same as that described in detail in an earlier publication.[14] As mentioned earlier, measurements were made both in toluene at room temperature and in benzene at 30 °C. In general, the maximum solution concentration was chosen such that the chain center-to-center spacing was roughly equal to or greater than twice the radius of gyration, R_G, of the chain in solution. In the case of the two highest molecular weight samples in benzene, the maximum concentrations were slightly higher than this, but no consequent effect was apparent in the results (see Table II). In all cases, the product of the magnitude of the scattering wave vector, K, and R_G was less than about 0.6—well below the value where internal modes of chain motion might interfere with chain center-of-mass diffusive motion as reflected in the autocorrelation spectrum (ACS).[5] For PCS measurements, the laser power at the sample varied between about 80 and 225 mW while the photodetection count rate varied between about 50 000 and 130 000. The scattering angle was varied between 30 and 60° while the correlator sample time setting ranged between 1 and 5 μs. The quality factor for these experiments, that is the ratio of the zero delay of the ACS value above the base line to the base line, ranged from about 0.1 to about 0.4.

Sample $\bar{M}_w$ values and solution second virial coefficient values (A_2) were measured in spectroscopic grade toluene at room temperature (21–23 °C), using a Chromatix KMX-6 low-angle laser (6328 Å) light scattering photometer.

The number-averaged molecular weights of six of the seven samples were measured in toluene at 39 °C in a Knauer Model 2001-A membrane osometer while that of the lowest molecular weight sample was made in toluene at room temperature in a Knauer Model 1001-A vapor pressure osometer. These $\bar{M}_n$ measurements were made at ArRo Laboratories (Joliet, Ill.). For comparison purposes, molecular weights relative to polystyrene of six of the samples were also determined by gel permeation chromatography (GPC) at ASI, Inc. (Santa Clara, Calif.). The molecular weight measurement results are presented in Table I.

Data Analysis

The PCS results presented in this paper are based on unclipped intensity autocorrelation spectra for self-beat experiments. These spectra may be represented by an expression of the form[15]

$$G^{(2)}(\tau) = A|G^{(1)}(\tau)|^2 + B \tag{6}$$

where $G^{(2)}(\tau)$ and $|G^{(1)}(\tau)|$ are the intensity and field autocorrelation functions, respectively, A is a proportionality constant incorporating the effect on the spectrum of partial coherence in the scattered light, and B is the spectral base line. With the approach explained in detail in ref 14, the logarithm of the base line corrected spectrum for any given experimental run was fit to a quadratic equation of the form

$$\ln |G^{(1)}(\tau)| = d + b\tau + a\tau^2 \tag{7}$$

where $\langle D\rangle_z = -b/K^2$ and $\delta_z = 2a/b^2$, with $\langle D\rangle_z$ the z-averaged PαMS chain center-of-mass diffusion coefficient and δ_z and the relative dispersion about $\langle D\rangle_z$

$$\delta_z = (\langle D^2\rangle_z - \langle D\rangle_z^2)/\langle D\rangle_z^2 \tag{8}$$

$\langle D\rangle_z$ values were measured at four solution concentrations for each sample and the infinite-dilution values, $\langle D\rangle_z^0$, or

Table II
PCS Results

SAMPLE NO.	TOLUENE, 25°C $D_0 \cdot 10^7$ (cm²/sec)	TOLUENE, 25°C k_D^C (cm³/g)	TOLUENE, 25°C k_D^Φ	BENZENE, 30°C $D_0 \cdot 10^7$ (cm²/sec)	BENZENE, 30°C k_D^C (cm³/g)	BENZENE, 30°C k_D^Φ
1	19.55±0.18	1.12±0.30	0.47	19.88±0.28	---	---
2	10.67±0.05	4.63±0.30	1.20	10.65±0.11	4.67±1.98	1.21
3	6.10±0.02	13.5±0.4	1.84	6.02±0.02	14.5±0.4	1.98
4	4.76±0.07	19.7±24	2.02	4.80±0.05	20.8±1.4	2.13
5	2.77±0.02	46.0±1.8	2.53	2.74±0.12	52.2±1.0	2.87
6	1.80±0.02	88.9±4.9	2.69	---	---	---
7	1.61±0.02	105.3±7.2	2.81	1.58±0.07	101.4±1.6	2.71

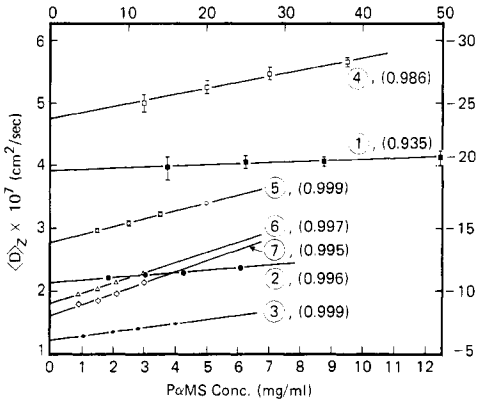

Figure 1. Plots of the z-averaged diffusion coefficient, $\langle D \rangle_z$, vs. polymer concentration, c. The left vertical and bottom horizontal axes refer to the open symbols while the right vertical and top horizontal axes refer to the solid. The circled numbers are the sample numbers while the numbers in parentheses are the linear correlation coefficients for each least-squares fit. Some points have no error bars because these are small enough to fit inside the symbol designating the point.

just D_0, were taken to be the intercept values from plots of $\langle D \rangle_z$ vs. concentration, c (see Table II and Figure 1). Ten spectra were taken at each concentration for each sample and the results presented in the tables and figures are the simple averages, with their standard deviations, of each set of ten measurements. Despite large uncertainties associated with their measurement, δ_z values for these samples indicated narrow molecular weight distributions[14] in agreement with the $\bar{M}_w/\bar{M}_n$ values determined by GPC and by TALS and osmometry. The δ_z values did not appear to depend on solution concentration. Typically, 55 points were used in each spectral fit.

For the time-averaged light scattering measurements, Kc/R_θ or, in some cases, $(Kc/R_\theta)^{1/2}$ vs. concentration, c, plots were very linear for all samples and were all fit to the standard equations for low scattering angles[16]

$$Kc/R_\theta = 1/\bar{M}_w + 2A_2c \tag{9}$$

or

$$(Kc/R_\theta)^{1/2} = 1/\bar{M}_w^{1/2}(1 + \bar{M}_w^{1/2}A_2c) \tag{10}$$

where

$$K = 2\pi^2n^2(\partial n/\partial c)^2(1 + \cos^2\theta)/\lambda^4N_A \tag{11}$$

with n the refractive index of toluene at 23 °C and 6328 Å (1.492), $\partial n/\partial c$ the specific refractive index increment for PαMS in toluene at room temperature (0.108), θ the scattering angle (4.35°), λ the vacuum wavelength of the laser light (6328 Å), and N_A Avogadro's number. R_θ is the excess Rayleigh factor. The $\bar{M}_w$ results are presented in Table I and the A_2 results are presented in Table IV.

Discussion of Results

The molecular weight measurement results are presented in Table I. Sample 6 was not measured by GPC and this is indicated in the table by dashes. To better assess the molecular weights of samples 1 and 2, these were run a second time on a GPC column set designed to measure low molecular weight samples.[17] These results are presented in parentheses in the table. While the general agreement between the samples is good for samples 4–7 and resonable for samples 2 and 3, the PCS polydispersity results (not presented) and the GPC results indicate that for samples 3–7, $\bar{M}_w/\bar{M}_n \lesssim 1.1$ and $\bar{M}_w/\bar{M}_n \simeq 1.2$ for sample 2. The molecular weight of sample 1 was more difficult to assess, but the TALS $\bar{M}_w$ result was found to be very reproducible and is probably the best single estimate of molecular weight for that sample. The polydispersity of sample 1 therefore lies in the range 1.4–1.6.

The PCS result are presented in Table II. The PCS polydispersity results are not shown because their statistical uncertainties are large and definitive $\bar{M}_w/\bar{M}_n$ values using the approach of ref 14 could not be calculated from them. The results are consistent with the polydispersity pattern described above, however. The excellent agreement between the toluene and benzene results for D_0 demonstrates the great precision and reproducibility of these measurements since according to the Stokes–Einstein expression, eq 4, the solution temperature and solvent viscosity effects should compensate to within 0.2%, which is well within experimental error. From Table II, it is seen that the sets of D_0 values do agree within the reported uncertainties. Moreover, the k_D values are in good agreement. Having two sets of independently determined k_D values proved useful in the analysis of the behavior of k_D. The errors reported in Table II are statistical uncertainties arising from least-squares fits to the $\langle D \rangle_z$ vs. concentration plots (Figure 1). The value of k_D for sample 1 is not reported because its statistical uncertainty was considered too large. As indicated by the dashes, sample 6 was not measured in benzene.

log–log plots of D_0 vs. $\bar{M}_n$ and $\bar{M}_w$ are presented in Figures 2 and 3. In Figure 2, $\bar{M}_n$ values are those obtained from osmometry while the $\bar{M}_w$ values were obtained by time-averaged light scattering. The corresponding plot using the GPC $\bar{M}_n$ and $\bar{M}_w$ results is presented in Figure 3.

The gradual change in slope with increasing sample molecular weight evident in Figures 2 and 3 corresponds to an increase in the magnitude of the power-law exponent

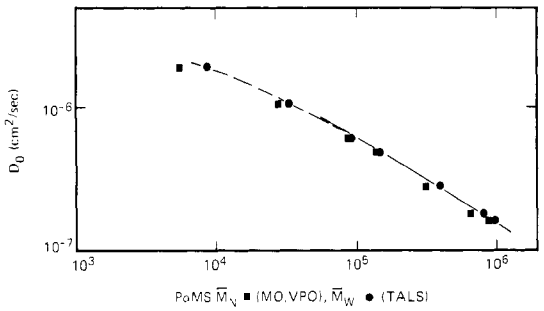

Figure 2. log–log plots of the z-averaged self-diffusion coefficient, D_0, vs. number-averaged molecular weight, $\bar{M}_n$, obtained by osmometry (solid squares) and vs. weight-averaged molecular weight, $\bar{M}_w$, obtained by time-averaged light scattering (solid circles).

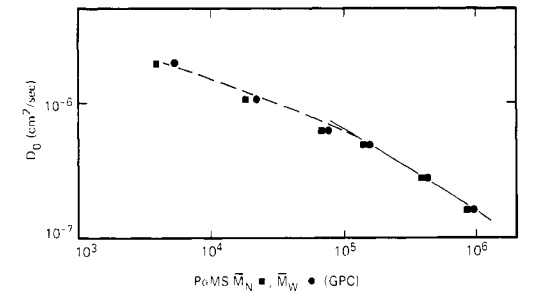

Figure 3. log–log plots of the z-averaged self-diffusion coefficient, D_0, vs. number-averaged molecular weight, $\bar{M}_n$ (solid squares), obtained by GPC and vs. weight-averaged molecular weight, $\bar{M}_w$ (solid circles), obtained by GPC.

Table III
D_0 vs. M Fits: $D_0 = CM^{-\nu}$ ($M > 10^5$)

$\bar{M}$	$C \cdot 10^4$	ν
$\bar{M}_W$, TALS	4.34±0.69	0.57±0.01
$\bar{M}_N$, MO	5.29±2.14	0.59±0.03
$\bar{M}_W$, GPC	6.08±2.94	0.60±0.04
$\bar{M}_N$, GPC	6.67±4.50	0.61±0.05

ν. The same behavior can also be found by using the GPC $\bar{M}_z$ results (see Table I). From the plots, it appears that the power-law parameters C and ν become constant above a molecular weight of about 10^5. Linear least-squares fits to the GPC, osmometry, and TALS ln D_0 vs. ln $\bar{M}$ plots for $M > 10^5$ show that, within the statistical uncertainty associated with these fits, both C and ν have attained constant values (see Table III).

The most reliable estimates of C and ν are obtained by averaging the three C and ν values that correspond to the three independently determined TALS, osmometry, and one of the GPC results. It can be shown that for narrow, symmetric molecular weight distribution samples such as samples 4–7, equivalent estimates of C and ν are obtained from fitting ln D_0 vs. ln $\bar{M}$ plots by using either $\bar{M}_n$ or $\bar{M}_w$. To show this, the effect of polydispersity on D_0 is calculated explicitly by expanding the z-averaged diffusion coefficient about $\bar{M}_n$ and $\bar{M}_w$, respectively. This type of calculation originated with the development of a method of using PCS to extract molecular weight information from dilute polymer solutions and explicit treatment of these expansions may be found in ref 18 and 14. For expansion about $\bar{M}_n$, the result is

$$D_0 = C\bar{M}_n^{-\nu}\frac{1 + [(2-\nu)(1-\nu)/2]\delta_{2n}}{1 + \delta_{2n}} \qquad (12)$$

$$\delta_{2n} = \bar{M}_w/\bar{M}_n - 1 \qquad (13)$$

Correspondingly, the expression for the expansion about $\bar{M}_w$ is

$$D_0 = C\bar{M}_w^{-\nu}\left\{1 - \frac{\nu(1-\nu)}{2}\left[\frac{\bar{M}_z}{\bar{M}_w} - 1\right]\right\} \qquad (14)$$

From eq 12 and 14, it is seen that for narrow, symmetric molecular weight distribution samples, the estimate of ν obtained from ln D_0 vs. ln $\bar{M}$ plots will be unaffected by polydispersity for expansion about either $\bar{M}_n$ or $\bar{M}_w$. The constant C, on the other hand, will be somewhat affected. More quantitatively, for $\nu = 0.59$ and $\bar{M}_z/\bar{M}_w = \bar{M}_w/\bar{M}_n = 1.1$, the corrections to C will be about 6% and 1% for expansion about $\bar{M}_n$ and $\bar{M}_w$, respectively. From the data presented in Table III, it is seen that these corrections are sufficiently smaller than the statistical uncertainties associated with the estimates of C that they may be ignored.

When expressions 12 and 14 are compared to the corresponding expression for expansion about $\bar{M}_z$, it is found that of the three molecular weight averages, plots of ln D_0 vs. ln $\bar{M}_w$ yield the minimum correction to C.[19] For this reason, the GPC $\bar{M}_w$ result along with the osmometry $\bar{M}_n$ and the TALS $\bar{M}_w$ results from Table III were averaged to obtain

$$D_0 = (5.24 \pm 0.48) \times 10^{-4}\bar{M}^{-0.59\pm0.01} \qquad (15)$$

Correspondingly

$$R_H = (7.49 \pm 0.69) \times 10^{-10}\bar{M}^{0.59\pm0.01} \qquad (16)$$

The uncertainties reported for C and ν are the standard deviations about their respective averages. The measured exponent, $\nu = 0.59$, is in good agreement with both the Flory prediction of $^3/_5$[1] and the recent renormalization group calculation of 0.588.[20]

Recalling the lower value of ν for polystyrene in a good solvent of room temperature over a similar molecular weight range, it is seen that methyl substitution in the backbone of polystyrene shifts the crossover between the Gaussian and excluded-volume regions, as observed in the hydrodynamic behavior, downward to a more accessible chain molecular weight range around 10^5.

The TALS measurements made in this study were made by using a low-angle photometer so R_G could not be measured. As mentioned earlier, R_G values for ten atactic, narrow-distribution PαMS samples in toluene at 25 °C were reported in ref 13. These samples ranged in molecular weight from 2×10^5 to 7.5×10^6 and were thus in the excluded-volume region. The measured polydispersities of these ten samples were very low: reportedly $\bar{M}_w/\bar{M}_n \leq 1.02$. From a least-squares fit to ln R_G vs. ln $\bar{M}_w$

$$R_G = (1.49 \pm 0.33) \times 10^{-9}\bar{M}_w^{0.58\pm0.01} \qquad (17)$$

The ratio R_H/R_G is therefore

$$R_H/R_G = 0.50 \pm 0.12 \qquad (18)$$

Note that the power-law exponent, to within experimental error, is the same for both R_H and R_G. This result, (18), is in reasonable agreement with the value of 0.537 predicted by Akcasu and Han for a linear chain in a good solvent.[7]

A value of $\nu = 0.59$ and the agreement of the measured R_H/R_G ratio with that predicted for a linear chain in a good solvent imply that for $M > 10^5$, PαMS in toluene at 25 °C has completed the transition into the excluded-volume region. Further evidence consistent with this implication is obtained by considering the measured second virial coefficients for these samples. In general, A_2 may be written[21]

$$A_2 = 4\pi^{3/2}N_A R_G^3\psi/M^2 \qquad (19)$$

Table IV

SAMPLE NO.	$A_2 \cdot 10^4$ (cm^3/g^2)	Ψ	$\bar{S}/R_H$
1	6.63	0.158	0.85
2	4.40	0.143	0.98
3	3.16	0.139	1.00
4	2.85	0.141	1.02
5	2.21	0.143	1.06
6	1.76	0.136	1.02
7	1.70	0.138	1.03

with N_A Avogadro's constant and ψ a function which measures the effect on A_2 of the interpenetration of polymer chains in dilute solution. This dimensionless parameter, ψ, is referred as the interpenetration function and should be constant in the excluded-volume region. It is computed from expression 19

$$\psi = A_2M^2/4\pi^{3/2}N_AR_G^3 \quad (20)$$

By substituting the measured $\bar{M}_w$ dependence of R_G and A_2 in the excluded-volume region, the constancy of ψ can be tested. A linear least-squares fit of log A_2 to log $\bar{M}_w$ yields

$$A_2 \sim \bar{M}_w^{-(0.28\pm0.01)} \quad (21)$$

in excellent agreement with the corresponding dependence

$$A_2 \sim \bar{M}_w^{-(0.29\pm0.01)} \quad (22)$$

from a fit to the data of Kato et al.[13] Substituting the R_G and A_2 dependences on $\bar{M}_w$ into expression 20 for ψ results in

$$\psi \sim \bar{M}_w^{-0.02} \quad (23)$$

This result shows that, within experimental uncertainty, ψ is constant in the excluded-volume region, as expected. In addition, explicit calculations of ψ for each PαMS sample, using eq 20, were made and are presented in Table IV. For samples 4–7 ($M > 10^5$), ψ fluctuates only slightly and has a value of $\psi = 0.140 \pm 0.003$. A recent paper on the calculation of ψ includes a compendium of the predictions of the value of ψ by a number of workers.[22] The value of $\psi = 0.140$ is in reasonable agreement with the predicted value of 0.18 of Fixman, Cassassa, and Markowitz (see also ref 21) and the recent predictions of 0.169 and 0.114 of Burch and Moore[23] (see also Table 1 of ref 22) although it is somewhat lower than the value of about 0.19 measured by Kato et al.[13]

It has been noted that when ψ is constant, the form of A_2 in eq 19 is that of a hard sphere[21]

$$A_2 = \frac{4N_AV}{M^2} = \frac{16\pi N_A}{3M^2}\bar{S}^3 \quad (24)$$

with V and $\bar{S}$ the hard-sphere volume and radius, respectively. This equivalence in form is consistent with the fact that polymer chains in a good solvent behave thermodynamically as noninterpenetrating spheres. This situation is analogous to the hydrodynamic case in which the chain, for the purposes of dynamics considerations, may be replaced by its equivalent Stokes' sphere.

By equating A_2 in expressions 19 and 24, as has been done previously,[7] the relationship between the equivalent hard-sphere radius $\bar{S}$ and the chain radius of gyration, R_G, is found to be

$$\bar{S} = \left(\frac{3\pi^{1/2}}{4}\psi\right)^{1/3}R_G \quad (25)$$

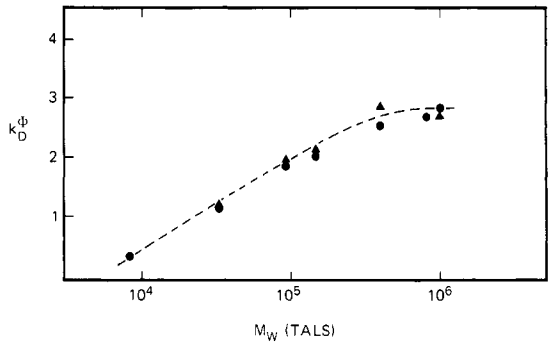

Figure 4. Plot of the chain–chain hydrodynamic interaction parameter, k_D^Φ (chain concentration in volume fraction units), for both toluene (solid circles) and benzene (solid triangles) vs. the weight-averaged molecular weight, $\bar{M}_w$, determined by light scattering.

It is interesting to compare the sizes of the two equivalent spheres. From Table IV, it is seen that for PαMS in the excluded-volume region, $\bar{S}/R_H = 1.03 \pm 0.02$ so that the equilvalent thermodynamic sphere is about 10% larger by volume than its hydrodynamic counterpart.

Next, the behavior of the diffusion coefficient second virial coefficient, k_D, is considered. This parameter may be written in terms of its thermodynamic and hydrodynamic parts as[21]

$$k_D = 2A_2M - k_f - \bar{v} \quad (26)$$

with $\bar{v}$ the polymer partial specific volume and k_f the frictional coefficient virial coefficient

$$f = f_0(1 + k_fc + ...) \quad (27)$$

and

$$D_0 = k_BT/f_0 \quad (28)$$

so that

$$f_0 = 6\pi\eta_0R_H \quad \text{(eq 4)} \quad (29)$$

Experimentally, k_D is extracted from the slope of the $\langle D\rangle_z$ vs. concentration curve (Figure 1, Table II) using eq 3. There are a host of predictions for the value of k_D for a nonionic solute in solution. These generally treat the solute either as a uniform hard sphere or, in the case of polymers, as a coil where the "hardness" of the equivalent sphere as a function of solvent power may or may not be considered (see ref 21, for example). In a good solvent in the excluded-volume region, a coiled linear chain can be considered to behave, as discussed earlier, both thermodynamically and hydrodynamically as its equivalent hard sphere.

It is easiest to assess which, if any, of the predictions of k_D is valid by expressing the concentration in eq 3 in volume fraction units (k_D^Φ) rather than in mass concentration units (k_D^c). Conversion between the corresponding interaction parameters is accomplished by using the expression[21]

$$k_{D,f}^\Phi = \frac{M}{N_AV_H}k_{D,f}^c \quad (30)$$

with V_H the hydrodynamic volume of the chain (see eq 33). Considering the measured k_D^Φ values for both toluene and benzene presented in Table II and Figure 4, it is seen that by using the $\bar{M}_w$ values, the limiting value of k_D^Φ is roughly 2.7. In the hard-sphere limit, k_D^Φ is variously predicted to be 0.84,[24] 1.2,[25] 2,[6,26] or 3[27] while for the derivation of Yamakawa[6,21,28]

$$k_D^\Phi = 3.2(\bar{S}/R_H)^3 - 1 \quad (31)$$

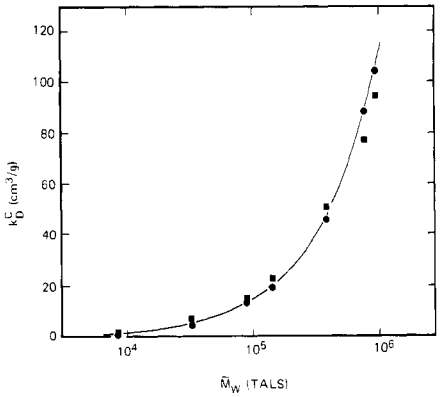

Figure 5. Plot of measured (solid circles) and calculated (solid squares) values of the chain–chain hydrodynamic interaction parameter, $k_D{}^c$ (mass concentration units), vs. the chain weight-averaged molecular weight, $\bar{M}_w$, determined by light scattering. The calculated values were computed by using the Yamakawa prediction for $k_f{}^c$ (eq 32). The curve is drawn freehand through the measured values.

This result is derived from the expression for $k_D{}^c$ given in eq 26 and is then converted to volume fraction units. In this derivation, $k_f{}^c$ is that given by Yamakawa for a coiled linear chain in a good solvent

$$k_f{}^c = 1.2A_2M + N_AV_H/M \tag{32}$$

and A_2 is given by eq 24. Again, V_H is the chain hydrodynamic volume

$$V_H = \tfrac{4}{3}\pi R_H{}^3 \tag{33}$$

In the excluded-volume region, the chain molecular weights are sufficiently large that the effect of $\bar{v}$ on $k_D{}^\Phi$ in eq 31 is negligible and is therefore ignored.

Using a value of $\bar{S}/R_H$ of 1.03 ± 0.02 for samples 4–7 (see Table IV), the Yamakawa treatment predicts

$$k_D{}^\Phi = 2.50 \pm 0.19 \tag{34}$$

in best agreement with the observed value of about 2.7.

A graphical comparison of the observed and the Yamakawa predictions of $k_D{}^c$ for samples 1–7 in toluene is presented in Figure 5. The value of $\bar{v}$ used in these calculated values ($\bar{v}$ must be considered for the lower molecular weight sample) is 0.873 as reported by Noda et al.[29] for PαMS in toluene at 25 °C. Again, at the higher molecular weights (e.g., samples 4–7) $\bar{v}$ may be ignored in these calculations.

Acknowledgment. Particular thanks are due to P. M. Cotts, who made the time-averaged light scattering measurements. Thanks are also due to K. Mittal, N. Eib, and L. Rosen for generously supplying samples, to D. Y. Yoon for pointing out the availability of the poly(α-methylstyrene) samples, and to D. W. Schaefer and A. C. Ouano for worthwhile discussions about the contents of this paper.

References and Notes

(1) Flory, P. J. "Principles of Polymer Chemistry"; Cornell University Press: Ithaca, N.Y., 1953; Chapter XIV.
(2) de Gennes, P. G. *Nature (London)* **1979**, *282*, 367.
(3) Stockmayer, W. H.; Albrecht, A. C. *J. Polym. Sci.* **1958**, *32*, 215.
(4) Weill, G.; des Cloizeaux, J. *J. Phys. (Paris)* **1979**, *40*, 99.
(5) Berne, B. J.; Pecora, R. "Dynamic Light Scattering—With Applications to Chemistry, Biology and Physics"; Wiley: New York, 1976; Chapter 8.
(6) Akcasu, A. Z.; Benmouna, M. *Macromolecules* **1978**, *11*, 1193.
(7) Akcasu, A. Z.; Han, C. C. *Macromolecules* **1979**, *12*, 276.
(8) Akcasu, A. Z.; Benmouna, M.; Han, C. C. *Polymer*, in press.
(9) Adam, M.; Delsanti, M. *J. Phys. (Paris)* **1976**, *37*, 1045.
(10) Schaefer, D. W.; Joanny, J. F.; Pincus, P. *Macromolecules* **1980**, *13*, 1280.
(11) Appelt, B.; Meyerhoff, G. *Macromolecules* **1980**, *13*, 657.
(12) Lyerla, J.; Horikawa, T. IBM Research Laboratory, San Jose, Calif., unpublished results.
(13) Kato, T.; Miyaso, K.; Noda, I.; Fujimoto, T.; Nagasawa, M. *Macromolecules* **1970**, *3*, 777.
(14) Selser, J. C. *Macromolecules* **1979**, *12*, 909.
(15) Koppel, D. E. *J. Chem. Phys.* **1972**, *57*, 4814.
(16) Reference 1, Chapter VII.
(17) Mathias, D. IBM Research Laboratory, San Jose, Calif., unpublished results.
(18) Pusey, P. N. In "Industrial Polymers: Characterization by Molecular Weight"; Green, J. H. S., Dietz, R., Eds.; Transcripta Books: London, 1973.
(19) This fact was pointed out by one of the referees of this paper.
(20) LeGuillou, J. C.; Zinn-Justin, J. *Phys. Rev. Lett.* **1977**, *39*, 95.
(21) Yamakawa, H. "Modern Theory of Polymer Solutions"; Harper and Row: New York, 1971; Chapter 4.
(22) Witten, T. A., Jr.; Schäfer, L. *J. Phys. A* **1978**, *11*, 1843.
(23) Burch, D. J.; Moore, M. A. *J. Phys. A* **1976**, *9*, 435.
(24) Pyun, C. W.; Fixman, M. *J. Chem. Phys.* **1964**, *41*, 935.
(25) Burgers, J. M. *Proc. Acad. Sci. Amsterdam* **1942**, *45*, 126.
(26) Altenburger, A. R.; Deutch, J. M. *J. Chem. Phys.* **1973**, *59*, 89.
(27) Harris, S. *J. Phys. A* **1976**, *9*, 1895.
(28) Yamakawa, H. *J. Chem. Phys.* **1962**, *36*, 2995.
(29) Noda, I.; Mizutani, K.; Kato, T.; Fujimoto, T.; Nagasawa, N. *Macromolecules* **1970**, *3*, 787.